Relativistic DFT Study on the Reaction Mechanism of Second-Row Transition Metal Ru with CO_2

Xian-Yang Chen, Yi-Xin Zhao, and Shu-Guang Wang*

School of Chemistry and Chemical Technology, Shanghai Jiao Tong University, Shanghai, 200240, China

Received: June 20, 2005; In Final Form: November 24, 2005

To estimate the importance of relativistic effects on the reaction mechanisms between Ru and CO_2, the potential energy surfaces have been performed in the triplet and quintet electronic states using quasi-relativistic (Pauli), zero-order regularly approximated (ZORA), and nonrelativistic (NR) density functional theory (DFT) at the PW91/TZP level. The results demonstrate that there are two rival reaction mechanisms: one is an addition mechanism and the other is an insertion mechanism in the triplet state. The only mechanism in the quintet state is the insertion mechanism. The most favored reaction mechanism in Ru + CO_2 is that the Ru atom in its ground state first attacks the CO bond of CO_2, forming q-Ru(CO)O ($^5A''$) with the insertion mechanism, and then undergoes an intersystem crossing to t-Ru(CO)O ($^3A''$). Then it crosses t-TS3 to produce t-ORuCO molecule. The relativistic effects are important for reactivity of the second-row transition metal to CO_2. In the key step of t-Ru(CO)O via t-TS3 to t-ORuCO, relativistic effects reduce the barrier energy by 10.3 kcal/mol, which is nearly half the nonrelativistic barrier energy.

1. Introduction

The use of carbon dioxide as an alternative precursor in organic synthesis has long been a challenge in synthetic chemistry. Under normal conditions, carbon dioxide is one of the most thermodynamically stable and inert triatomic molecules due to the large C═O bond energy. Therefore, its activation and conversion into useful organic compounds requires a huge amount of energy input. The energy to activate CO_2 molecule can be substantially reduced by catalysts. Among these catalysts, transition metal complexes have a higher potential than others,[1] and the coordination of CO_2 with a transition metal atom is thought to be a key step in this process. To understand how various metal atoms can react with CO_2 and what the reaction mechanisms in the catalytic processes are, several articles have been reviewed.[2−4] Many matrix isolation UV−visible and infrared spectroscopic experiments have been carried out for a series of first-row transition metal (from Sc to Cu)/CO_2 systems.[5−11] These investigations showed that there are very different reaction mechanisms between the late transition metal atoms [Fe, Co, Ni, and Cu] and the early ones [Sc, Ti, V, and Cr]. The late transition metals may form M(CO_2) complexes, whereas the early ones may insert into a CO bond yielding OMCO species.[13] The OMCO species either decompose to MO + CO or form OM(CO_2) and OMCO(CO_2) by fixation of another CO_2 molecule. Much theoretical research[12−23] has been published concerning the reactions of first-row transition metals with CO_2 molecule, and the results predicted were in good agreement with the experimental results.

Meanwhile, the reactions of several heavier transition metals (M = Zr, Ta, Mo, Ru, Os, W, U, Th) with CO_2 have been recently investigated[24−30] by matrix infrared spectroscopy in combination with some theoretical calculations. These studies showed that the heavier metals are easier to insert into a CO bond yielding OMCO species, and decomposed compounds were not observed. This demonstrates from experiment results that there are great differences between the first-row transition metals and late heavier metals in their ability to react with CO_2 molecule. However, little theoretical work has been done regarding their detailed reactive mechanisms. The difficulty of theoretical investigation in reaction mechanism with heavier transition metals is due to correlation effects and relativistic effects.

Here we want to present a detailed study of the reaction mechanism in the gas phase of ruthenium atom with CO_2 at the triplet and quintet states. The aim of this paper is to answer two questions: first, we want to know the reactive mechanism in detail is and why ORuCO compound is not easily decomposed to RuO + CO, similar to the insertion products produced by early first-row transition metals. Second, we want to find out how important the relativistic effects are in the reaction process, especially at the transition state. Only a few have been reported: for example, Bickelhaupt et al.[31] reported relativistic effects on the oxidative addition reactions of palladium to CH_3-Cl, CH_4, and C_2H_6. Density functional calculations were performed to optimize all stable species and transition states with and without relativistic correction.

2. Theoretical Calculations

All calculations were performed using a relativistic density functional theory (DFT) program of the Amsterdam density functional (ADF2004) package initially developed by Baerends et al.[32−34] In this work, the density functional used was based on the model, the Vosko−Wilk−Nusair (VWN)[35] local-spin-density correlated potential, and the gradient corrections of the exchange correlation of Perdew and Wang[36] (PW91). Several other density functionals such as the Becke nonlocal exchange correction and the Becke−Perdew (BP) nonlocal exchange correlation corrections were also tested. There is not much difference between VWN-BP and VWN-PW91. The frozen-core approximation was adopted for C ($1s^2$), O ($1s^2$), and Ru

* To whom correspondence should be addressed. E-mail: sgwang@sjtu.edu.cn.

10.1021/jp053296+ CCC: $33.50 © 2006 American Chemical Society
Published on Web 02/21/2006

TABLE 1: Energy Differences[a] between Ground and Excited Electronic States of Ru

state	chosen Slater determinant[b]	Pauli + PW91	ZORA + PW91	PW91	expt[c]
^{5}F	$\|(5s)^1(4d_0)^2(4d_{\pm1})^2(4d_2)^2(4d_{-2}\alpha)^1\|$	0.0	0.0	0.0	0.0
^{3}F	$\|(5s\beta)^1(4d_0)^2(4d_{\pm1})^2(4d_2)^2(4d_{-2}\alpha)^1\|$	19.1	18.9	16.8	18.0
^{5}D	$\|(5s)^2(4d_0)^2(4d_{\pm1})^2(4d_{\pm2}\alpha)^2\|$	24.5	27.2	43.2	20.0

[a] Relative energies in kcal/mol with respect to Ru(^{5}F). [b] In D_∞ symmetry. [c] From ref 43.

TABLE 2: ZPE-Corrected Energies Relative to Ru(^{3}F) + CO_2 (kcal/mol) of Various Compounds and Transition States at the TZP Basis Sets

molecule	Pauli + PW91	ZORA + PW91	PW91
Ru(^{3}F) + CO_2	0.0	0.0	0.0
t-RuOCO, ^{3}A″	−8.7	−8.5	−15.5
t-cyc-$RuCO_2$, ^{3}A″	2.6	4.7	5.5
t-ORuOC, ^{3}A″	−8.8	−5.8	−2.9
t-Ru(CO)O, ^{3}A″	−36.0	−36.0	−38.4
t-ORuCO, ^{3}A″	−62.1	−58.4	−50.6
RuO($^3\Pi$) + CO	8.0	11.3	7.9
t-TS1, ^{3}A″	5.6	2.5	9.2
t-TS2, ^{3}A″	11.2	13.2	13.4
t-TS3, ^{3}A″	−28.6	−25.6	−20.7
Ru(^{5}F) + CO_2	−19.1	−18.9	−16.8
q-Ru(CO)O, ^{5}A″	−29.6	−26.4	−21.5
q-ORuCO, ^{5}A″	−46.0	−42.2	−33.5
q-TS, ^{5}A″	−7.1	−4.1	0.7
q-RuO($^5\Delta$) + CO	−5.3	−2.1	2.6

TABLE 3: Vibrational Frequencies (cm^{-1}) of Various Compounds and Transition States Calculated at the PW91/TZP Level with Pauli Correction

molecule	frequencies (cm^{-1})
t-RuOCO, ^{3}A″	65.7, 106.9, 195.1, 443.3, 1250.5, 2352.1
t-cyc-$RuCO_2$, ^{3}A″	325.2, 417.6, 459.1, 770.7, 928.7, 1071.1
t-ORuOC, ^{3}A″	88.9, 225.1, 229.1, 337.3, 911.8, 1864.9
t-Ru(CO)O, ^{3}A″	292.2, 401.8, 446.9, 706.3, 925.4, 1817.1
t-ORuCO, ^{3}A″	156.1, 414.7, 451.3, 548.3, 883.0, 1957.3
t-TS1, ^{3}A″	687.0i, 349.8, 353.1, 474.1, 1051.7, 1332.1
t-TS2, ^{3}A″	370.2i, 207.4, 351.3, 460.7, 746.4, 1590.4
t-TS3, ^{3}A″	499.5i, 349.5, 367.7, 544.5, 717.7, 1935.8
q-Ru(CO)O, ^{5}A″	182.7, 289.5, 513.8, 640.5, 1124.1, 1868.9
q-ORuCO, ^{5}A″	75.5, 333.6, 337.3, 418.0, 829.0, 1979.8
q-TS, ^{5}A″	498i, 294.2, 304.7, 497.6, 646.1, 1948.6

$(1s^2-3d^{10})$. The core electrons were calculated by the accurate relativistic Dirac−Slate method[37] and then transferred unchanged into the molecules. The valence orbitals of C, O, and Ru used triple-ζ Slater-type orbital (STO) with one additional d/p polarization function STO basis set (TZP).[38] The relativistic corrections were carried out by the most popular scalar relativistic Pauli formalism,[39] which contains mass−velocity and Darwin effects, and a newly developed zero-order regular approximation, i.e., the ZORA method.[40] Equilibrium and transition state structures were fully optimized. Harmonic frequencies were calculated by numerical differentiation of the energy gradients. The vibrational zero point energy (ZPE) corrections were based on the corresponding frequency calculation.

To analyze reaction path characters, the minimum energy path (MEP) was followed in both directions (forward and backward) using the intrinsic reaction coordinate (IRC)[41,42] at the level of PW91/TZP with Pauli relativistic corrections, on the transition state located at the same theoretical level.

3. Results and Discussion

The excited state energies relative to the ground state of Ru atom are shown in Table 1. Table 2 presents the ZPE-corrected energies of various compounds and transition states in the triplet and quintet states reaction paths relative to Ru(^{3}F) + CO_2. Table 3 presents the vibrational frequencies, and Table 4 gives the Mulliken charge and spin density on Ru atom of various compounds and transition states in the Ru (^{3}F and ^{5}F) + CO_2 system calculated at the Pauli-PW91/TZP level. Structure parameters of various compounds and transition states are shown in Figure 1. Figure 2 provides the triplet and quintet potential energy diagrams along the reaction pathways computed at the Pauli-PW91/TZP level. Figure 3 gives the Mulliken orbital populations of Ru atom along reaction routes with and without Pauli relativistic correction. To demonstrate the importance of relativity on reaction routes, relativistic energy changes in potential energy surfaces are presented in Figure 4.

3.1. Energy Splitting between Electronic States of Ru Atom. According to experimental atomic spectra[43] and spin−orbit averaged values, the lowest excited triplet and quintet states of the Ru atom are $4d^75s^1$ (^{3}F) and $4d^65s^2$ (^{5}D), which lie above the quintet $4d^75s^1$ (^{5}F) ground state by 18.0 and 20.0 kcal/mol, respectively. The calculated excitation energies of Ru atom are shown in Table 1. Due to the shortage of present-day DFT for representing atomic degenerate densities, we used Baerends method[44] to evaluate the ground, first, and second excited states of Ru. The lowest energy of Ru(^{5}F) obtained for the occupation of the d orbital is $(4d_0)^2(4d_{\pm1})^2(4d_2)^2(4d_{-2}\alpha)$.[1] The energy of this determinant is lower than fractional occupation by 6.9 kcal/mol at the Pauli-PW91/TZP level. The lowest energies of the ^{3}F and ^{5}D states obtained are $(5s\beta)^1(4d_0)^2(4d_{\pm1})^2(4d_2)^2(4d_{-2}\alpha)^1$ and $(5s)^2(4d_0)^2(4d_{\pm1})^2(4d_{\pm2}\alpha)$,[2] respectively. The difference between ^{3}F and the ground state ^{5}F is only one s electron turned from α to β. In this excitation, there are no d−s electron promotions, so the nonrelativistic calculations may reproduce its energy. PW91 gives only 1.2 kcal/mol error; meanwhile, Pauli-PW91 overestimates it by 1.1 kcal/mol and ZORA-PW91 overestimates it by 0.9 kcal/mol. The second lower lying state is ^{5}D, in which one d electron from the ground state is excited to the s orbital. It is well-known that relativistic effects stabilize the s electron and destabilize the d electron. When one d electron is excited to the s orbital, forming the ^{5}D state, the relativistic effects play an very important role. PW91 could not give the correct energy prediction without relativistic corrections. After relativistic corrections, the excitation energy errors may be overcome by ~80%. The excitation energies of ^{3}F and ^{5}D from ^{5}F are only overestimated 1.1 and 4.5 kcal/mol by PW91/TZP with the Pauli correction compared to experiments, respectively, whereas the ZORA correction overestimates the excited energies of ^{5}D from ^{5}F by 7.2 kcal/mol. Therefore, we think PW91/TZP with the Pauli correction is suitable to reproduce the various electronic states of Ru atom. In this paper, we will use the Pauli-PW91 method at the TZP level to describe the reactive mechanisms of the Ru/CO_2 system.

3.2. Reaction Mechanism in the Triplet State Ru(^{3}F). The ground state of Ru atom is ^{5}F ($4d^75s^1$); however, the experimental observed ground state of ORuCO is an electronic triplet state. The difference in energy between triplet and quintet states of ORuCO from Pauli, ZORA, and nonrelativistic PW91 of DFT calculations are −16.1, −16.2, and −17.1 kcal/mol, respectively (see Table 2). At the Pauli-PW91/TZP level, we also calculated the ^{3}A′ state of t-ORuCO and obtained 33.9 kcal/mol higher

TABLE 4: Mulliken Charges and Spin Density on Ru Atom of Various Compounds and Transition States in Ru/CO_2 System Calculated at the Pauli-PW91/TZP Level

molecule	q_{Ru}	q_{O1}	q_{O2}	q_C	spin density on Ru atom
CO_2		−0.46	−0.46	0.92	
t-RuOCO, $^3A''$	0.06	−0.46	−0.51	0.90	2.06
t-TS1, $^3A''$	0.55	−0.50	−0.56	0.52	2.46
t-cyc-$RuCO_2$, $^3A''$	0.66	−0.51	−0.51	0.36	2.0
t-TS2, $^3A''$	0.73	−0.45	−0.59	0.31	1.74
t-ORuOC, $^3A''$	0.70	−0.58	−0.35	0.23	1.60
t-Ru(CO)O, $^3A''$	0.49	−0.48	−0.56	0.55	2.01
t-TS3, $^3A''$	0.61	−0.39	−0.57	0.35	1.73
t-ORuCO	0.75	−0.58	−0.36	0.18	1.55
RuO($^3\Pi$), $^3A''$	0.53	−0.53			1.69
RuO($^5\Delta$), $^5A''$	0.59	−0.59			3.27
q-Ru(CO)O, $^5A''$	0.39	−0.47	−0.54	0.62	3.87
q-TS, $^5A''$	0.64	−0.36	−0.57	0.29	3.28
q-ORuCO, $^5A''$	0.75	−0.31	−0.59	0.15	2.91

than the $^3A''$ state and also 17.8 kcal/mol higher than that of q-ORuCO ($^5A''$) in energy. Therefore, we will not discuss the $^3A'$ potential energy surface.

As seen in Figures 1 and 2, similarly to Sc(^{2}D) + CO_2,[14] Ti(^{3}F) + CO_2,[13] and Ni(^{3}F) + CO_2[21] reactions, two mechanisms are possible for Ru(^{3}F) + CO_2, which can be called insertion and addition mechanisms. At the initial reaction step in the addition route, the Ru(^{3}F) attacks CO_2 from the oxygen side of the molecule, and a planar adduct intermediate t-RuOCO ($^3A''$) is spontaneously formed without any barrier. This is different from Sc(^{2}D) + CO_2, Ti(^{3}F) + CO_2, and Ni(^{3}F) + CO_2 reactions. There is an entrance barrier in Sc(^{2}D) + CO_2, and no adduct MOCO compound has been found in Ti(^{3}F) + CO_2 and Ni(^{3}F) + CO_2 reactions. As seen from Figure 1, in the t-RuOCO intermediate, the Ru−O bond length is greater than 2.1 Å and the CO_2 fragment is very little distorted compared to the free molecule. The stabilization energy of the complex t-RuOCO is 8.7 kcal/mol lower than that of reactants Ru(^{3}F) + CO_2 at the PW91/TZP level with Pauli correction. From the t-RuOCO intermediate, the reaction proceeds to produce the t-cyc-$RuCO_2$ ($^3A''$) molecule via transition state t-TS1. The Ru−O bond in t-TS1 is slightly shrunk by 0.05 Å compared to that in t-RuOCO, while the RuOC angle is smaller to 92.5° and the OCO angle becomes bent to 116.2°. The t-cyc-$RuCO_2$ isomer is a nearly C_{2v}-symmetric $\eta^2_{O,O}$-coordination model of Ru atom toward CO_2, and the binding energy between Ru(^{3}F) and CO_2 is about −2.6 kcal/mol. There is nearly no energy difference between the $^3A_2$ (C_{2v}) and $^3A''$ states. Therefore, we will use the t-cyc-$RuCO_2$ $^3A''$ state to hold the symmetry consistent. IRC calculations at the Pauli-PW91/TZP level confirmed that t-TS1 is connected to t-cyc-$RuCO_2$ ($^3A''$) in the forward direction. The IRC pathway in the reversed direction led to the initial addition complex t-RuOCO, and not to the reactants, Ru(^{3}F) + CO_2. The Pauli-PW91/TZP calculated barrier height and endothermicity of the t-RuOCO ($^3A''$) → t-cyc-$RuCO_2$ ($^3A''$) reaction step are 14.3 and 11.3 kcal/mol, respectively. From t-cyc-$RuCO_2$ ($^3A''$), the reaction proceeds to produce the t-ORuOC ($^3A''$) via transition state t-TS2 with 8.6 kcal/mol barrier and releasing heat about 11.4 kcal/mol. One of the C−O bonds changes from 1.326 Å in the t-cyc-$RuCO_2$ to 1.864 Å in the transition state. This indicates the C−O bond starts to be broken. The end Ru−O bond length in the t-ORuOC ($^3A''$) isomer is only 0.028 Å longer than that in free RuO($^3\Pi$) molecule, whereas the end C−O bond is also only 0.028 Å longer than that in free CO molecule. The t-ORuOC ($^3A''$) isomer can decompose to RuO($^3\Pi$) + CO without any barrier and with endothermicity of 16.8 kcal/mol.

To understand the electronic details of the reaction from t-RuOCO ($^3A''$) to t-ORuOC ($^3A''$), we have analyzed the orbital interactions along the series of reaction steps, which are shown in Figure 3a and Table 4. This route consists of two reaction steps: t-RuOCO ($^3A''$) → t-TS1 → t-cyc-$RuCO_2$ ($^3A''$) and t-cyc-$RuCO_2$ ($^3A''$) → t-TS2 → t-ORuOC ($^3A''$). The former involves large structural change and significant electronic reorganizations due to endothermicity. The positive charge of Ru rapidly increases from 0.06*e* in t-RuOCO ($^3A''$) to 0.66*e* in t-cyc-$RuCO_2$ ($^3A''$), and this corresponds to the rapid decrease of Ru 4d electrons from 7.46 to 6.73. However, the maximum of the Ru 5s population lies in t-TS1. This shows that the main source of donated electrons comes from the Ru 4d orbital, and not the 5s orbital. The latter is an exothermic reaction step accompanied by a lesser charge transfer. As a whole reaction route, the positve charge of Ru is maximized around t-TS2 and the maximum of the spin density on the Ru lies in t-TS1. Thus, the donated electrons of Ru mainly come from 4d orbital.

The second pathway is an insertion mechanism. The triplet Ru atom attaches to the C−O bond in carbon dioxide with the formation of a planar $\eta^2_{C,O}$-coordination model of t-Ru(CO)O ($^3A''$) without any barrier. To find the transition state that connects Ru(^{3}F) + CO_2 and t-Ru(CO)O ($^3A''$), we have scanned the potential energy surface restricted Ru−C distances from 4.0 to 2.0 Å and optimized all other geometry parameters. The energy is monotonically decreased to that of t-Ru(CO)O ($^3A''$). Such a case is also shown in the Ti(^{3}F) insertion in CO_2 to form Ti(CO)O.[13] The intermediate t-Ru(CO)O has a quite high stabilization by 36.0 kcal/mol relative to Ru(^{3}F) + CO_2. The attacked C−O bond in t-Ru(CO)O intermediate is elongated to 1.34 Å, and the OCO angle is changed from 180° to 138° at the Pauli-PW91/TZP level. The reason that the CO_2 fragment is so distorted compared to free CO_2 is 0.49*e* transferred from Ru atom to the diffuse lobe of C′ 2p orbital in bent CO_2, and the negatively charged CO_2 can stabilize in a bent structure. This case results in the C−O bond starting to weaken and lengthen because of the antibonding character. From t-Ru(CO)O intermediate, the reaction proceeds to produce the product t-ORuCO ($^3A''$) via transition state t-TS3, which is confirmed by IRC calculation. This reaction step has 7.4 kcal/mol barrier height and 26.1 kcal/mol exothermicity. The C−O bond in t-TS3 compared to that in t-Ru(CO)O is further elongated to 1.75 Å; Ru−O and Ru−C distances are further shortened by about 0.1 Å. t-ORuCO is very stable with 62.1 kcal/mol lower than that of the initial reactants, while Liang and Andrews reported[30] that t-Ru(CO)O was only lower than that of Ru atom and CO_2 by 1.8 kcal/mol. The large difference between our result and Andrews' is that (i) they did not point out the electronic state of Ru atom and (ii) their calculation was with small GTO basis sets of LANL2DZ (ECP) on Ru. In this reaction route, the oxygen abstraction and metal insertion take place simultaneously with the electron transfer to CO_2. The amount of electron

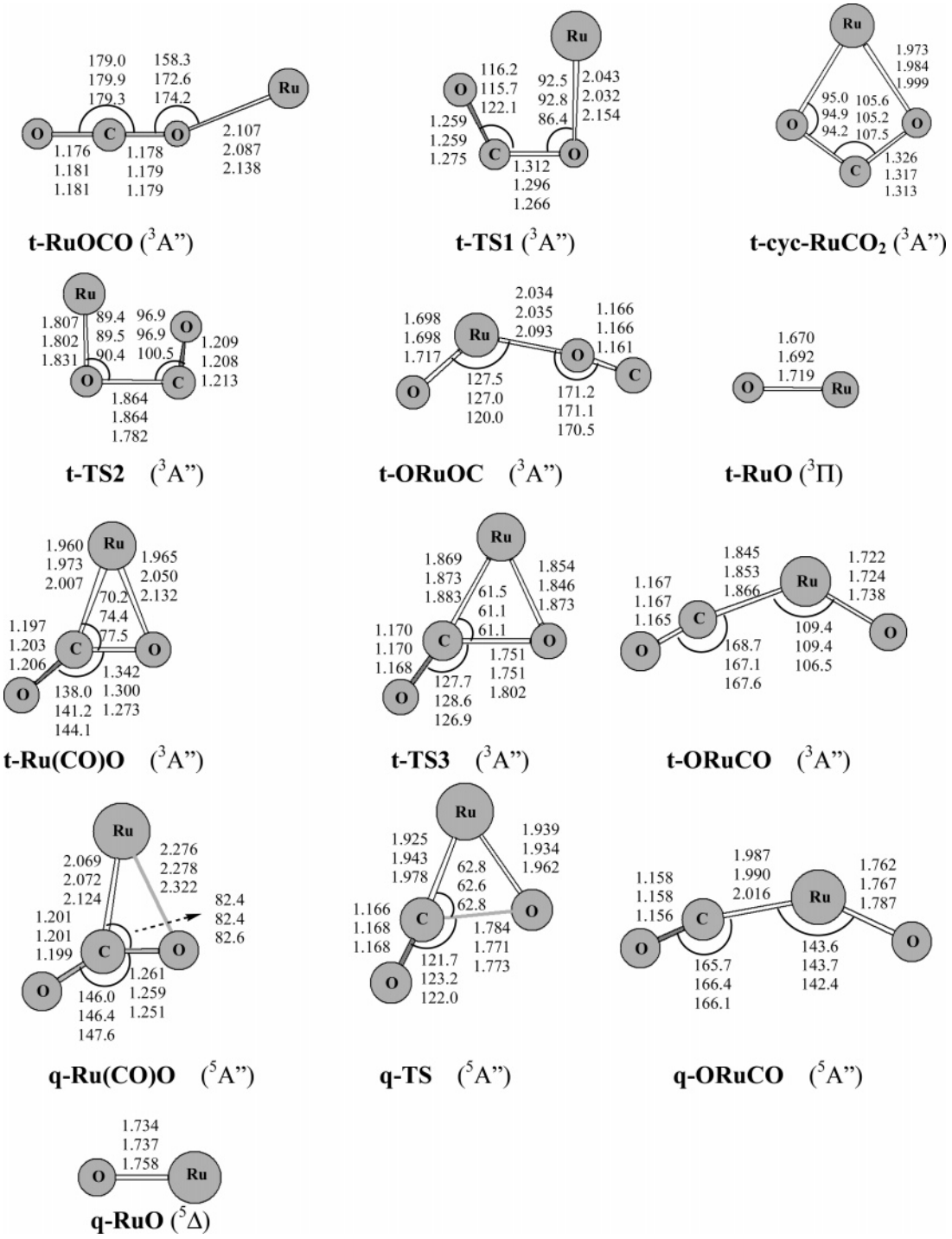

Figure 1. Optimized geometries for intermediates, products, and transition states (bond lengths in angstroms and bond angles in degrees). Values from top to bottom: Pauli + PW91/TZP, ZORA + PW91/TZP, and PW91/TZP, respectively.

transfer monotonically increases from 0.49*e* on Ru in t-Ru(CO)O to 0.75*e* in t-ORuCO; this is consistent with decreasing 4d orbital populations of Ru as the reaction proceeds. Therefore, the donated electrons of Ru atom also mainly come from the 4d orbital.

Comparing the insertion and addition reactions of the Ru(^{3}F) + CO_2 system, it seems that the two rival reaction routes form the two initial intermediates (t-RuOCO and t-Ru(CO)O) spontaneously. In fact, the insertion reaction should be favored either thermodynamically or kinetically. Although t-RuOCO is easily formed with an exothermicity of 8.7 kcal/mol, it is difficult to pass across t-TS1 to produce t-cyc-$RuCO_2$ due to the high barrier required, 14.4 kcal/mol. t-Ru(CO)O is more easily formed with a high stability of 36.0 kcal/mol, and the exothermic energy is enough to overcome a barrier of 7.4 kcal/mol to produce t-ORuCO. Apparently, only t-ORuCO can be detected experimentally in this reaction. t-cyc-$RuCO_2$ is not easily detected experimentally due to its thermodynamic unstability: it is 2.6 kcal/mol higher than the initial reactants (Ru(^{3}F) + CO_2). Also, it requires only 3.0 kcal/mol to cross the t-TS1 barrier to return to the intermediate t-RuOCO and 8.6 kcal/mol to cross the t-TS2 barrier to produce t-ORuOC. Therefore, the Ru(^{3}F) + CO_2 reaction is not likely to follow the addition mechanism via this intermediate at low temperatures. For the reverse RuO($^3\Pi$) + CO reaction, the most possible product is also t-ORuCO because it can be formed without any

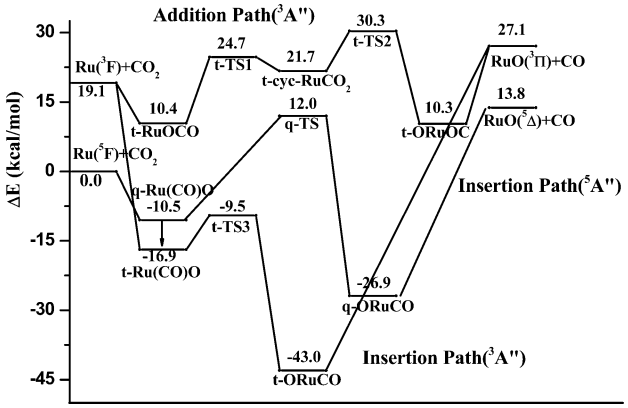

Figure 2. Potential energy surface of Ru + CO_2 reaction paths in triplet and quintet electronic states at DFT Pauli-PW91/TZP level.

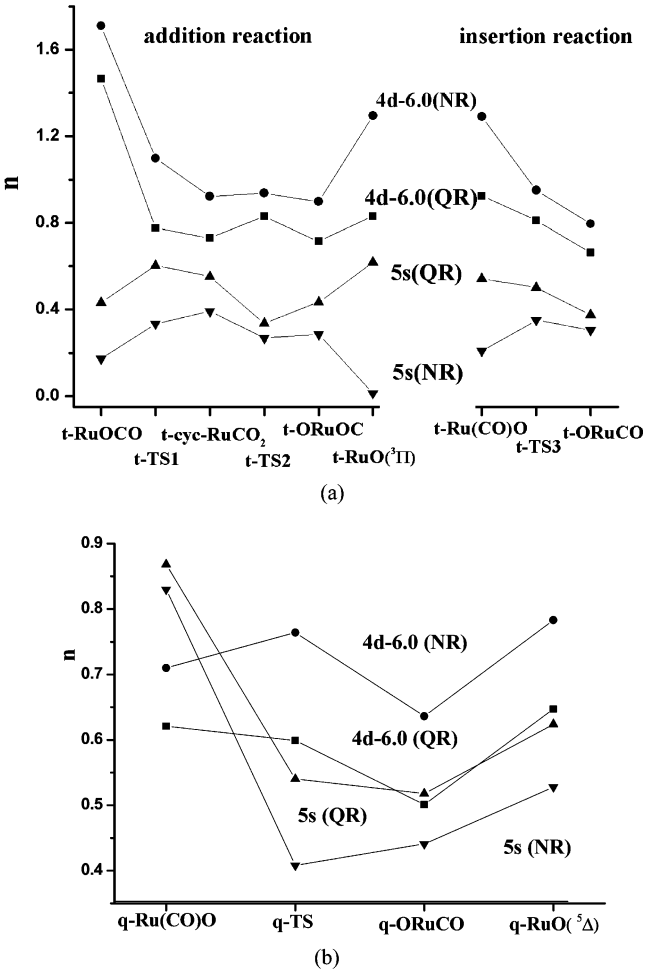

Figure 3. Atomic orbital population *n* of Ru along reaction paths. (a) Triplet state; (b) quintet state. QR, quasi-relativistic (Pauli); NR, nonrealtivistic.

barrier and with an exothermicity of 70.1 kcal/mol, and t-ORuCO is more stable than t-ORuOC by 53.3 kcal/mol. Thus, the t-ORuOC species is also not likely to be detected in experiment.

3.3. Reaction Mechanism in the Quintet State Ru(^{5}F). It is different from the reactive mechanisms of triplet state Ru atom and CO_2 molecule, and also different from the first-row transition metal reaction with CO_2. We could not find the addition mechanism that involves quintet state Ru atom. Only the insertion path has been found. For quintet state Ru atom, there are two electronic states: one is the ground state ^{5}F ($4d^7$-

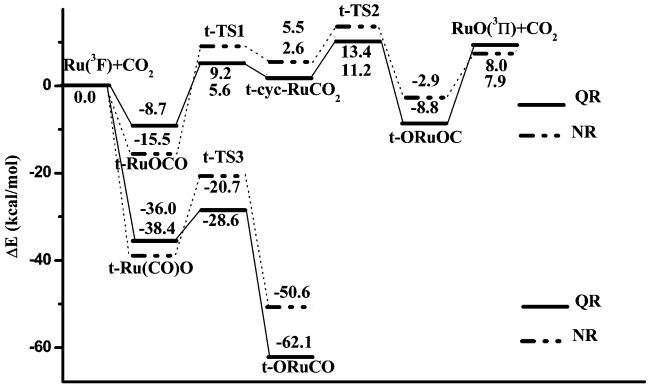

(a) Triplet state

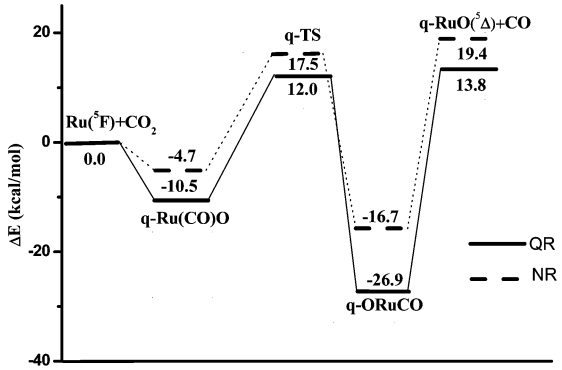

(b) quintet state

Figure 4. Relativistic effects in potential energy surfaces of Ru-(^{3}F) + CO_2 reaction (a) and Ru(^{5}F) + CO_2 reaction (b) at PW91/TZP level. Path A, addition mechanism; path B, insertion mechanism. QR, quasi-relativistic (Pauli); NR, nonrelativistic.

$5s^1$), and the other is the second excited state ^{5}D ($4d^65s^2$). Although the ground state (^{5}F) is stabilized by 20 kcal/mol more than the excited state (^{5}D), it could not directly point out which electronic state will take part in the reaction process. Therefore, we have analyzed orbital populations of Ru along the insertion mechanism process (shown in Figure 3). The populations of 5s are less than 1.0*e*, and populations of 4d are more than 6.5*e*, so we can judge that it is the ground state ^{5}F Ru atom that takes part in the insertion mechanism.

Similarly to the triplet state insertion mechanism, Ru(^{5}F) atom first attacks one of the C═O bonds in the CO_2 molecule to form $\eta^2_{C,O}$-Ru(CO)O (^{5}A″) intermediate. The transition structure related to Ru(^{5}F) + CO_2 and q-ORuCO could not be found. Intermediate q-Ru(CO)O (^{5}A″) is 10.5 kcal/mol lower than the reactant Ru(^{5}F) + CO_2 energetically. This is less pronounced than the triplet state t-Ru(CO)O, which is lower than the triplet state reactants by 36.0 kcal/mol. Further, distortion of the CO_2 fragment in the q-Ru(CO)O structure is also less pronounced than that in t-Ru(CO)O compared to free CO_2. The C−O bond is only elongated to 1.261 Å, and the OCO angle is bent to 146.0°. The reason is that there is only 0.39*e* (presented in Table 4), which is less than that in t-Ru(CO)O by 0.49*e*, transferred from quintet state Ru atom to the $3\pi^*$ orbital of CO_2 molecule, so the CO_2 fragment requires a small distortion to be stabilized. From q-Ru(CO)O (^{5}A″) intermediate the reaction proceeds to produce the q-ORuCO (^{5}A″) via transition state (q-TS, ^{5}A″) with a barrier of 22.5 kcal/mol. This barrier height is obviously higher than that of the triplet state insertion reaction, which only has 7.4 kcal/mol. IRC calculation confirmed that q-TS connects

q-Ru(CO)O ($^5A''$) and q-ORuCO ($^5A''$). The exothermicity of the q-Ru(CO)O ($^5A''$) → q-ORuCO ($^5A''$) step is 16.4 kcal/mol; then 40.7 kcal/mol should be required if q-ORuCO ($^5A''$) decomposes to RuO($^5\Delta$) + CO.

Finally, we relate our results to the experimental evidence from a matrix isolation study.[30] In this experimental study one of the products formed in the reactions of laser ablated Ru atoms with CO_2 was identified as the ORuCO insertion complex. Its three absorption bands in the argon matrix are 1966.1, 836.1, and 509.0 cm^{-1}, which are assigned to C−O stretching, Ru−O stretching, and Ru−CO stretching modes, respectively. These bands do not change following annealing, indicating that ORuCO is difficult to decompose thermodynamically to RuO + CO. This is consistent with our calculations (shown in Table 3) that the C−O, Ru−O, and Ru−CO stretching frequencies of t-ORuCO are 1957.3, 883.0, and 548.3 cm^{-1}, respectively. Although the C−O and Ru−O stretching frequencies (1979.8 and 829.0 cm^{-1}) calculated in q-ORuCO show a close resemblance to the experimental observation, there is a 91.0 cm^{-1} difference in the Ru−CO stretching frequencies (418.0 cm^{-1}) between the calculated results and the experimental values. Therefore, t-ORuCO is the only feasible product for the title reaction corresponding to the triplet state insertion mechanism.

Alternatively, there is also another pathway in the Ru(^5F) + CO_2 reaction. When the intermediate q-Ru(CO)O ($^5A''$) is formed, it may undergo an intersystem crossing by its vibrational motion to the t-Ru(CO)O ($^3A''$) state. The harmonic vibrational model of 640.5 cm^{-1} is that Ru and O move close to each other and C moves far from O. This distortion is close to the geometry of t-Ru(CO)O intermediate; that is, R_{Ru-O} is 0.311 Å shorter and R_{Ru-C} is 0.081 Å longer in t-Ru(CO)O than in q-Ru(CO)O states. t-Ru(CO)O is 6.4 kcal/mol lower than q-Ru(CO)O energetically. Then, reaction proceeds from t-Ru(CO)O via transition state (t-TS3) to produce the product t-ORuCO ($^3A''$).

3.4. Relativistic Effects. Relativistic effects play an important rule in heavy atomic systems. To understand the changes by relativistic effects of the Ru + CO_2 system, we have made a comparison between the relativistic and nonrelativistic cases at the PW91/TZP level. As shown in Figure 1, there is not much difference in the geometries of various compounds and transition structures on both the triplet and quintet states between Pauli and ZORA relativistic corrections. The maximum difference in bond length is only 0.04 Å in t-Ru(CO)O ($^3A''$). From Table 2, we find less than 4 kcal/mol differences between the Pauli and ZORA methods in energies. Both Pauli and ZORA formalisms give the same reaction mechanisms qualitatively. To see the relativistic effects in this system, we choose Pauli relativistic corrections to compare the relativistic and nonrelativistic results which can use the same STO basis sets.

As shown in Figure 4, relativistic effect does not always stablilize species in the triplet state addition and insertion mechanisms. Comparing with nonrelativistic results, relativity makes the initial forming complexes unstable with respect to the separate reactants Ru(^3F) + CO_2. For example, relativity destabilizes the t-RuOCO complex by 6.8 kcal/mol and t-Ru(CO)O by 2.4 kcal/mol. For the decomposed compounds (RuO($^3\Pi$) + CO), there is no difference in stability between the Pauli correction and nonrelativity. In the addition process of Ru(^3F) + CO_2, relativistic effect stabilizes t-TS1 and t-TS2 by 3.6 and 2.2 kcal/mol, respectively. In the insertion process, relativistic effect stabilizes t-TS3 and t-ORuCO by 7.9 and 11.5 kcal/mol, respectively. It is well-known that the 5s orbital is stabilized by the relativistic mass−velocity effect and 4d orbital is destabilized by the so-called "indirect effect" which is caused by relativistic change of the core electron distribution. This is in good agreement with the cases of the change in Ru's 5s and 4d populations along the reaction paths shown in Figure 3.

Ru attacks CO_2 to form the initial complex t-RuOCO ($^3A''$) in the addition pathway by induced-dipole−induced-dipole interaction between CO_2 and Ru. The magnitude of the effect depends on the size and the polarizability of the electron cloud of Ru atom. This makes the electron of 5s transfer to the 4d orbital in order to get more dispersion force. Relativistic effects reduce the energy gap of the 5s−4d orbital and increase the possibility of electron shifting. There is about 0.5*e* transferring to 4d from 5s orbital in t-RuOCO. The initial complex destabilized by relativistic effects due to more electrons on the 4d orbital and fewer electrons on the 5s orbital. In the t-TS1 state, Ru atom transfers 0.55*e* to CO_2, mostly coming from the 4d orbital of Ru. The transition state is stabilized by relativistic effect due to reduced 4d population in the Ru atom. Both sides decrease the activation barrier by 10.4 kcal/mol from the key step in the addition route from relativistic effects. Such a case also occurs in the insertion reaction route of Ru(^3F) + CO_2.

Different from the insertion reaction of the triplet state, relativistic effects stabilize all compounds and transition states in the insertion reaction of the quintet state. Relativistic effects stabilize the intermediate q-Ru(CO)O by 8.1 kcal/mol. The main reason relativistic effects stabilize q-Ru(CO)O and destabilize t-Ru(CO)O is that the Ru 4d electrons in q-Ru(CO)O are fewer by 0.2*e* than those in t-Ru(CO)O and 5s electrons in q-Ru(CO)O are more by 0.3*e* than those in t-Ru(CO)O. In the reaction process, Ru 4d electrons gradually deacrease; thus, relativity stabilizes q-TS by 6.4 kcal/mol and the product q-ORuCO by 12.5 kcal/mol. Because relativistic effects stabilize q-Ru(CO)O, the barrier of the insertion reaction of the quintet state is hardly affected by relativity.

It can be seen from Figure 1 that there are somewhat relativistic contractions of bonds that involve Ru atom, i.e., Ru−O and Ru−C bonds, in all cases in the triplet and quintet state reaction routes. The maximum relativistic bonding contraction appears in the Ru−O bond of t-Ru(CO)O by 0.167 Å, whereas t-Ru(CO)O is destabilized by relativistic correction. Upon comparison the bond lengths of Ru−O and Ru−C in the insertion route of the triplet state with those in the insertion route of the quintet state, it can be found that the relativistic contractions in the triplet state are less pronounced than those in the quintet state. For example, the Ru−O bond is shortened by 0.016 Å in t-ORuCO, 0.025 Å in q-ORuCO, 0.019 Å in t-TS3, and 0.023 Å in q-TS. The Ru−C bond is shortened by 0.021 Å in t-ORuCO, 0.029 Å in q-ORuCO, 0.014 Å in t-TS3, and 0.053 Å in q-TS. However, it can be seen from Figure 4 that the relativistic effects stabilized or destabilized the species in different cases. Therefore, there is no simple relation between the relativistic stability and bond contraction. In most cases relativistic effects cause the bond contractions involving the heavy atom Ru.

4. Conclusion

From the relativistic density functional investigation of Ru + CO_2 reaction mechanisms, we may draw the following conclusions:

1. There are two rival reaction channels from the reactants in triplet state: one is an addition mechanism; the other is an insertion mechanism. In the addition mechanism, t-RuOCO and t-ORuOC will be spontaneously formed as main products, whereas the amount of t-cyc-$RuCO_2$ will be small due to the high barrier required. The decomposition compounds RuO($^3\Pi$)

+ CO also will be small due to less stabilization. In the insertion mechanism, t-ORuCO will be the sole product; although t-Ru(CO)O is quite stable, it requires only 7.4 kcal/mol to cross the TS3 and to form the t-ORuCO product. Because the initial complex t-Ru(CO)O is of higher stabilization than the initial complex t-RuOCO by 27.3 kcal/mol, the insertion mechanism will be favored either thermodynamically or kinetically.

2. In the quintet state, we have only found the insertion mechanism of the Ru(^{5}F) atom into a CO bond forming $\eta^2_{C,O}$-Ru(CO)O (^{5}A″) via q-TS to produce the quintet state of ORuCO molecule with an exothermicity of 26.9 kcal/mol. The latter is not easy to dissociate to RuO($^5\Delta$) + CO due to the endothermicity of 40.7 kcal/mol required. From the q-Ru(CO)O intermediate, it also may go through an intersystem crossing to the t-Ru(CO)O species, which is 6.4 kcal/mol lower than the former quintet state in energy. Then it passes through the transition state t-TS3 to produce t-ORuCO.

3. Therefore, the most favored reaction mechanism in Ru + CO_2 is that the Ru atom in its ground state first attacks a CO bond of CO_2, forming q-Ru(CO)O (^{5}A″) with the insertion mechanism, and then undergoes an intersystem crossing to t-Ru(CP)O (^{3}A″) from the ground state to the excited state of Ru atom. Then it crosses t-TS3 to produce the t-ORuCO molecule.

4. The relativistic effects are important for the second-row transition metal ruthenium atom reaction with CO_2 molecule if we want to give an accurate quantum mechanical description. The 5s orbital of Ru is stabilized and the 4d orbital is destabilized by relativity. Although relativity does not significantly change the geometries of reaction species, it influences the energies observably. In the key step of t-Ru(CO)O via t-TS3 to t-ORuCO, relativistic effects reduce the barrier energy by 10.3 kcal/mol, which is nearly half the nonrelativistic barrier energy.

Acknowledgment. We acknowledge financial support from the National Science Foundation of the People's Republic of China (No. 20373014, No. 20573074).

References and Notes

(1) Braunstein, P.; Matt, D.; Nobel, D. *Chem. Rev.* **1988**, *88*, 747.
(2) Behr, A. *Angew. Chem., Int. Ed. Engl.* **1988**, *27*, 661.
(3) Jessop, P. G.; Ikariya, T.; Noyori, R. *Chem. Rev.* **1995**, *95*, 259.
(4) Gibson, D. H. *Chem. Rev.* **1996**, *96*, 2063.
(5) Mascetti, J.; Tranquille, M. *J. Phys. Chem.* **1988**, *92*, 2177.
(6) Leitner, W. *Coord. Chem. Rev.* **1996**, *153*, 257.
(7) Mascetti, J.; Galan, F.; Papai, I. *Coord. Chem. Rev.* **1999**, *190*−*192*, 557.
(8) Galan, F.; Fouassier, M.; Tranquille, M.; Mascetti, J.; Papai, I. *J. Phys. Chem. A* **1997**, *101*, 2626.
(9) Zhou, M.; Liang, B.; Andrews, L. *J. Phys. Chem. A* **1999**, *103*, 2013.
(10) Zhou, M.; Andrews, L. *J. Am. Chem. Soc.* **1998**, *120*, 13230.
(11) Zhou, M.; Andrews, L. *J. Phys. Chem. A* **1999**, *103*, 2066.
(12) Caballol, R.; Sanchez Marcos, E.; Barthelat, J. C. *J. Phys. Chem.* **1987**, *91*, 1328.
(13) Hwang, D. Y.; Mebel, A. M. *J. Chem. Phys.* **2002**, *116*, 5633.
(14) Hwang, D. Y.; Mebel, A. M. *Chem. Phys. Lett.* **2002**, *357*, 51.
(15) Papai, I.; Hannachi, Y.; Gwizdala, S.; Mascetti, J. *J. Phys. Chem. A* **2002**, *106*, 4181.
(16) Hannachi, Y.; Mascetti, J.; Stirling, A.; Papai, I. *J. Phys. Chem. A* **2003**, *107*, 6708.
(17) Jeung, G. H. *Mol. Phys.* **1989**, *67*, 747.
(18) Sodupe, M.; Branchadell, V.; Oliva, A. *J. Phys. Chem.* **1995**, *99*, 8567.
(19) Jeung, G. H. *Chem. Phys. Lett.* **1995**, *232*, 319.
(20) Papai, I.; Mascetti, J.; Fournier, R. *J. Phys. Chem. A* **1997**, *101*, 4465.
(21) Mebel, A. M.; Hwang, D. Y. *J. Phys. Chem. A* **2000**, *104*, 11622.
(22) Papai, I.; Schubert, G.; Hannachi, Y.; Mascetti, J. *J. Phys. Chem. A* **2002**, *106*, 9551.
(23) Pantazis, D. A.; Tsipis, A. C.; Tsipis, C. A. *Collect. Czech. Chem. Commun.* **2004**, *69*, 13.
(24) Souter, P. F.; Andrews, L. *Chem. Commun.* **1997**, 777.
(25) Souter, P. F.; Andrews, L. *J. Am. Chem. Soc.* **1997**, *119*, 5350.
(26) Wang, X. F.; Chen, M. H.; Zhang, L. N.; Qin, Q. Z. *J. Phys. Chem. A* **2000**, *104*, 758.
(27) Chen, M. H.; Wang, X. F.; Zhang, L. N.; Qin, Q. Z. *J. Phys. Chem. A* **2000**, *104*, 7010.
(28) Zhang, L. N.; Wang, X. F.; Chen, M. H.; Qin, Q. Z. *Chem. Phys.* **2000**, *254*, 231.
(29) Andrews, L.; Zhou, M., Liang, B.; Li, J.; Bursten, B. E. *J. Am. Chem. Soc.* **2000**, *122*, 11440.
(30) Liang, B.; Andrews, L. *J. Phys. Chem. A* **2002**, *106*, 4042.
(31) Diefenbach, A.; Bickelhaupt, F. M. *J. Chem. Phys.* **2001**, *115*, 4030.
(32) Baerends, E. J.; Ellis, D. E.; Ros, P. *Chem. Phys.* **1973**, *2*, 41.
(33) Velde, G.; Baerends, E. J. *J. Comput. Phys.* **1992**, *99*, 84.
(34) Ziegler, T.; Rauk, A.; Baerends, E. J. *Theor. Chim. Acta* **1977**, *43*, 261.
(35) Vosko, S. H.; Wilk, L.; Nusair, M. *Can. J. Phys.* **1980**, *58*, 1200.
(36) Perdew, J. P.; Chevary, J. A.; Vosko, S. H.; Jackson, K. A.; Pederson, M. R.; Singh, D. J.; Fiolhais, C. *Phys. Rev. B* **1992**, *46*, 6671.
(37) Rosen, A.; Lindgren, I. *Phys. Rev.* **1968**, *176*, 114.
(38) Snijders, G. J.; Baerends, E. J.; Vernooijs, P. *At. Data Nucl. Data Tables* **1982**, *26*, 483.
(39) Snijders, J. G.; Baerends, E. J.; Ros, P. *Mol. Phys.* **1979**, *38*, 1909.
(40) van Lenthe, E.; Baerends, E. J.; Snijders, J. G.. *J. Chem. Phys.* **1994**, *101*, 9783.
(41) Deng, L.; Ziegler, T.; Fan, L. *J. Chem. Phys.* **1993**, *99*, 3823.
(42) Deng, L.; Ziegler, T. *Int. J. Quantum Chem.* **1994**, *52*, 731.
(43) NIST Chemistry Webbook, NIST Standard Reference Data Base Number 69, http://physics.nist.gov/PhysRefData/Handbook/Tables/rutheniumtable5.htm.
(44) Baerends, E. J.; Branchadell, V.; Sodupe, M. *Chem. Phys. Lett.* **1997**, *265*, 481.